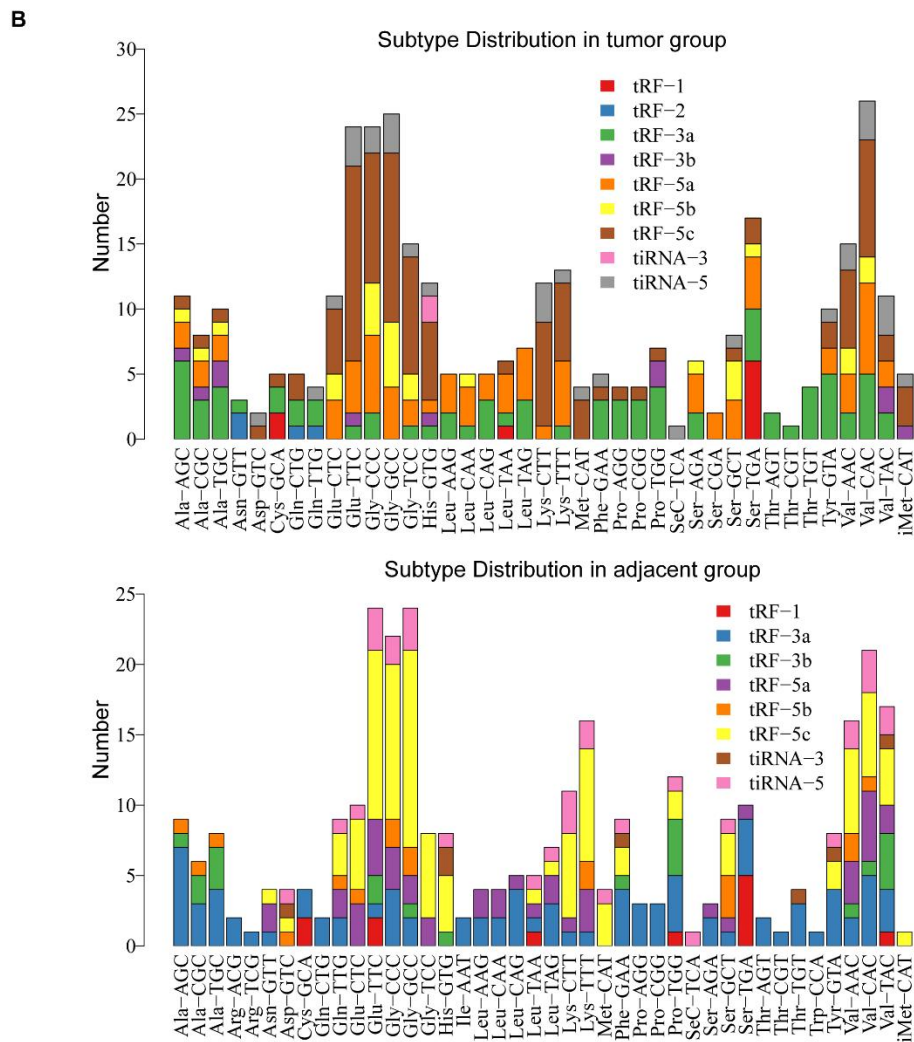
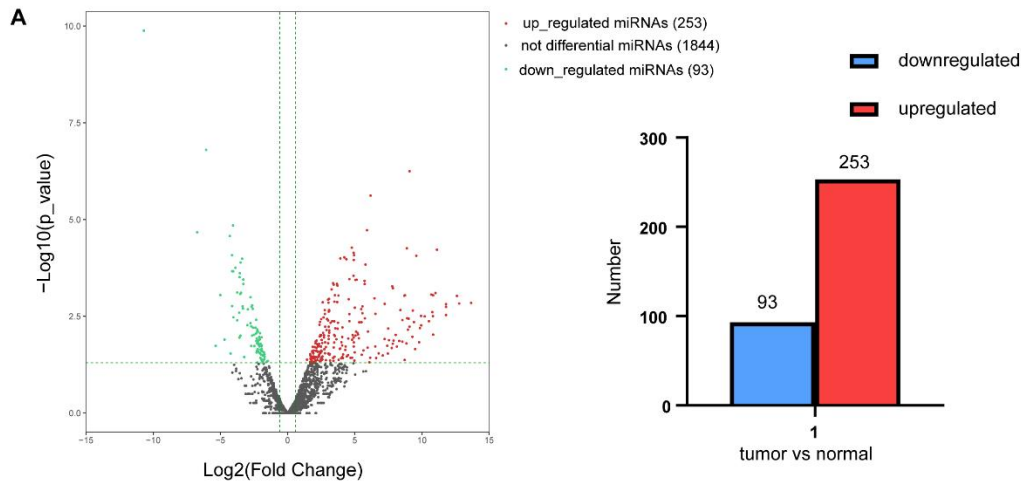


1 Supplementary Figures and Figure Legends

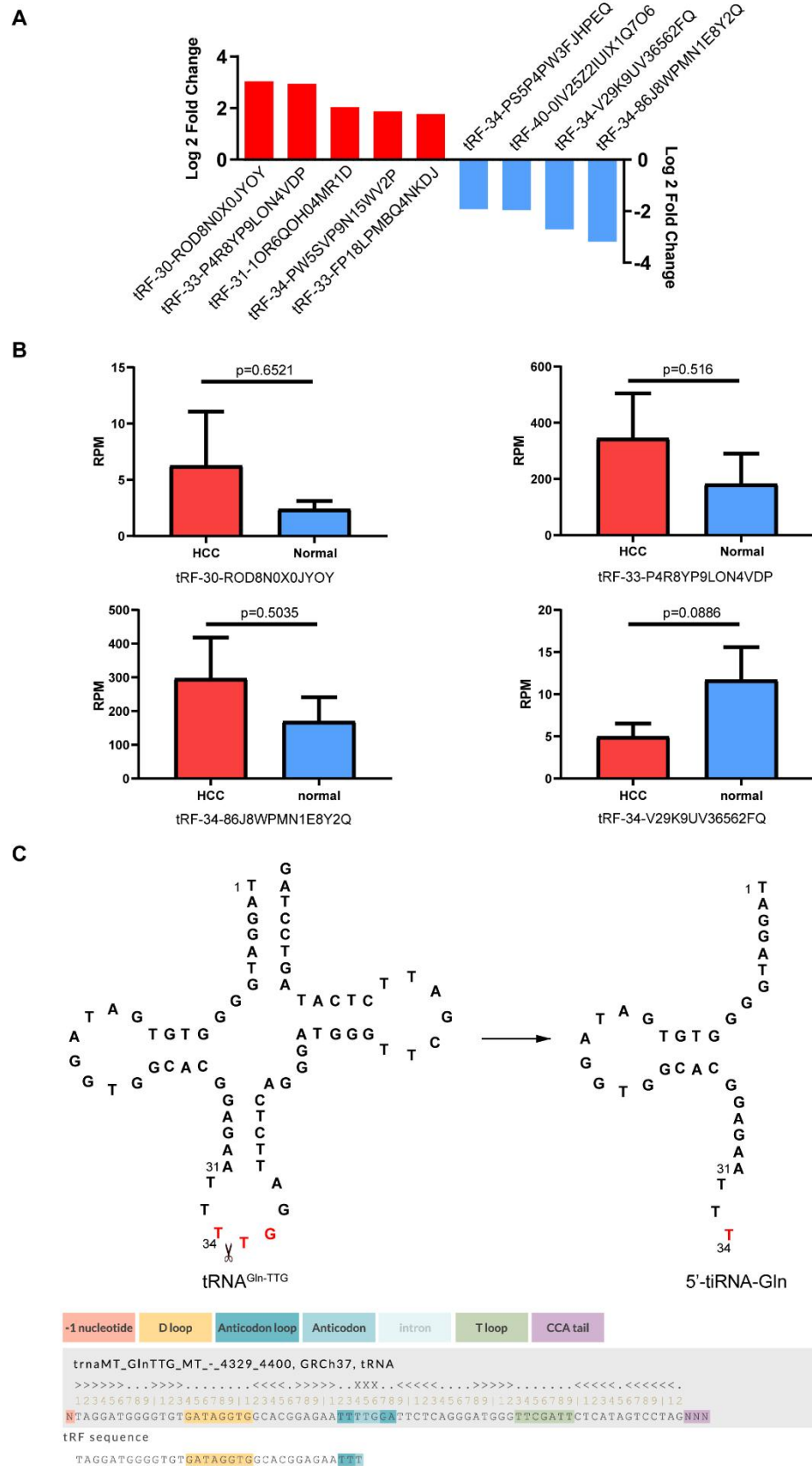


2

3

Supplementary Figure S1

4 **Supplementary Figure S1.** Differentially expressed miRNAs and subtype tsRNAs
5 against the tRNA isodecoders and isoacceptors. **A**, Left: Volcano plot of differentially
6 expressed miRNAs. Red: upregulated; green: downregulated. Right: The number of
7 down- or upregulated miRNAs in HCC tumor tissues as compared to the adjacent
8 nontumor tissues. Red: upregulated; blue: downregulated. **B**, The number of subtype
9 tsRNAs against the tRNA isodecoders and isoacceptors.

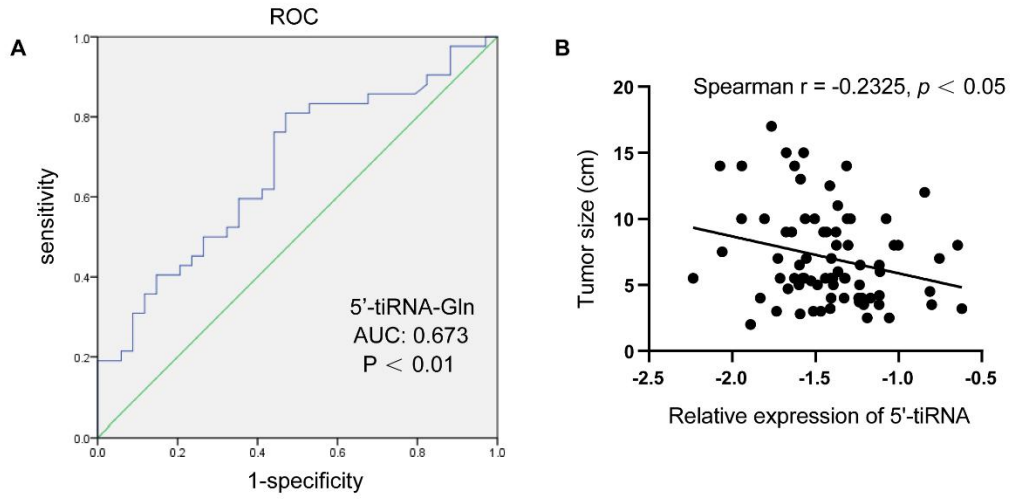


10

11

Supplementary Figure S2

12 **Supplementary Figure S2.** The sequence information of 5'-tiRNA-Gln and its
13 expression level from MINTbase. **A**, Differential expression of tiRNAs with
14 annotation in MINTbase in 4 pairs of HCC tumor tissues and adjacent nontumorous
15 tissues. **B**, tiRNAs expression data from MINTbase in HCC tumor tissues and normal
16 liver tissues. **C**, The cleavage site is located on the anticodon loop of tRNA^{Gln-TTG}.

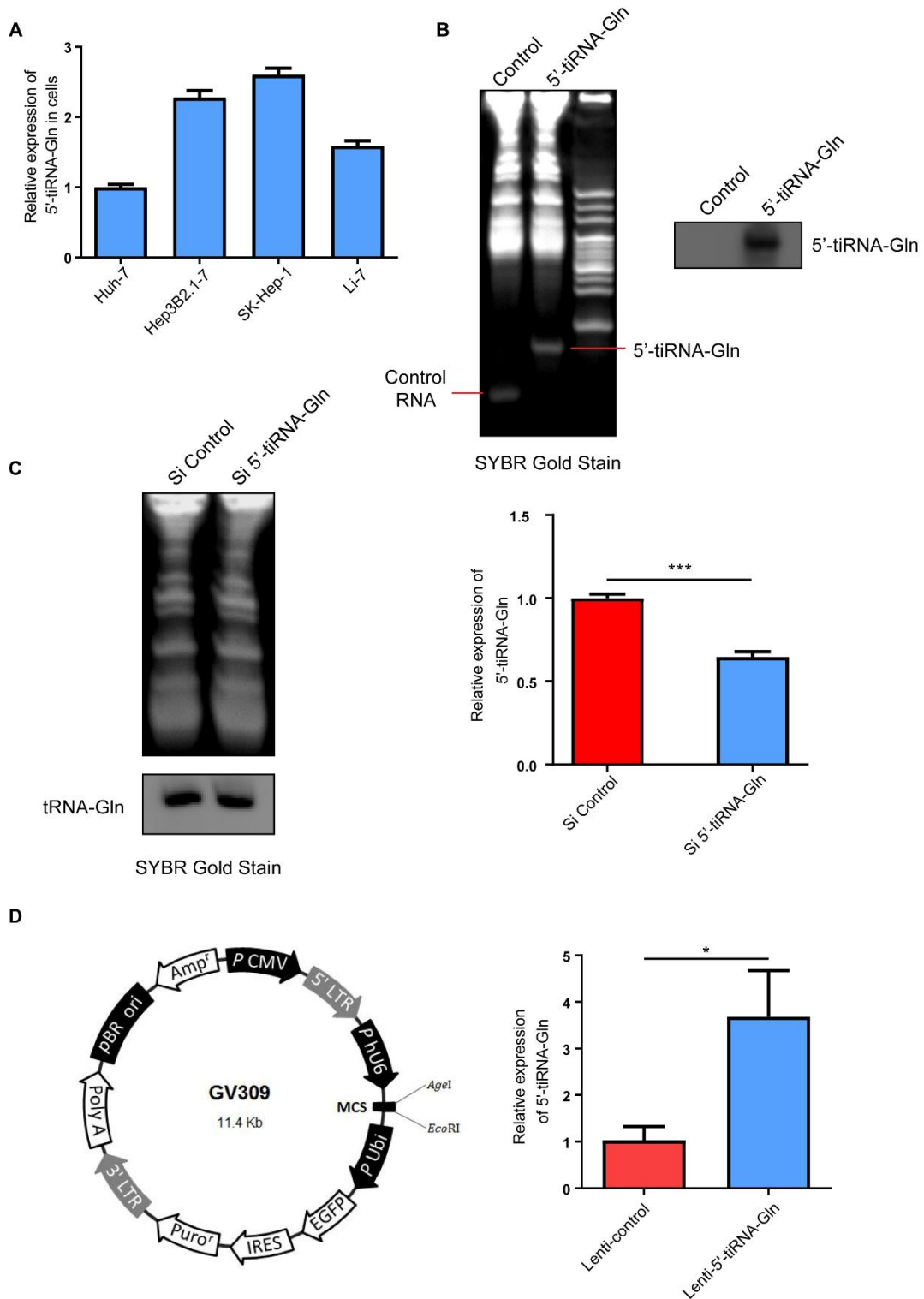


17

18

Supplementary Figure S3

19 **Supplementary Figure S3.** The correlation between the expression level of
20 5'-tiRNA-Gln and the clinical features. **A**, The ROC curve for 5' -tiRNA-Gln
21 including HCC metastasis patients and non-metastasis patients. **B**, The Spearman's
22 correlation analysis of the relationship between 5'-tiRNA-Gln and tumor size.

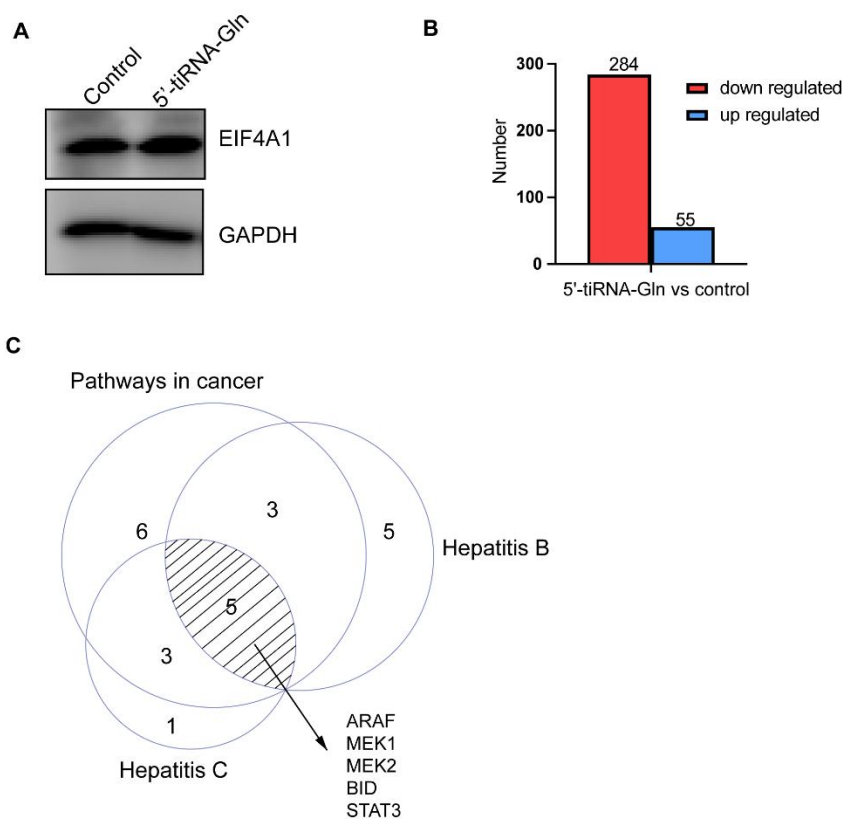


23

24

Supplementary Figure S4

25 **Supplementary Figure S4.** 5'-tiRNA-Gln expression levels in HCC cells. **A**, Relative
26 5'-tiRNA-Gln expression levels in HCC cells. **B**, Northern blotting detection of Huh-7
27 cells transfected with 5'-tiRNA-Gln or control RNA. Left: SYBR Gold staining of
28 15% urea-TBE PAGE; labels indicate the 5'-tiRNA-Gln and control RNA. Right:
29 DIG-labeled probe detection of 5'-tiRNA-Gln. **C**, Detection of tRNA-Gln and
30 5'-tiRNA-Gln levels in SK-Hep-1 cells transfected with Si-5'-tiRNA-Gln or Si-control.
31 Short exposure after SYBR Gold staining showed the total RNA loading; the
32 tRNA-Gln level was detected by the DIG-labeled probe. The efficiency of knockdown
33 by Si-5'-tiRNA-Gln was detected by RT-qPCR. **D**, Schematic diagram of the
34 lentivirus vector structure. Bar chart shows the expression level of Huh-7 cells
35 infected with lenti-5'-tiRNA-Gln as compared to the lenti-control. * $P < 0.05$, *** $P <$
36 0.001.

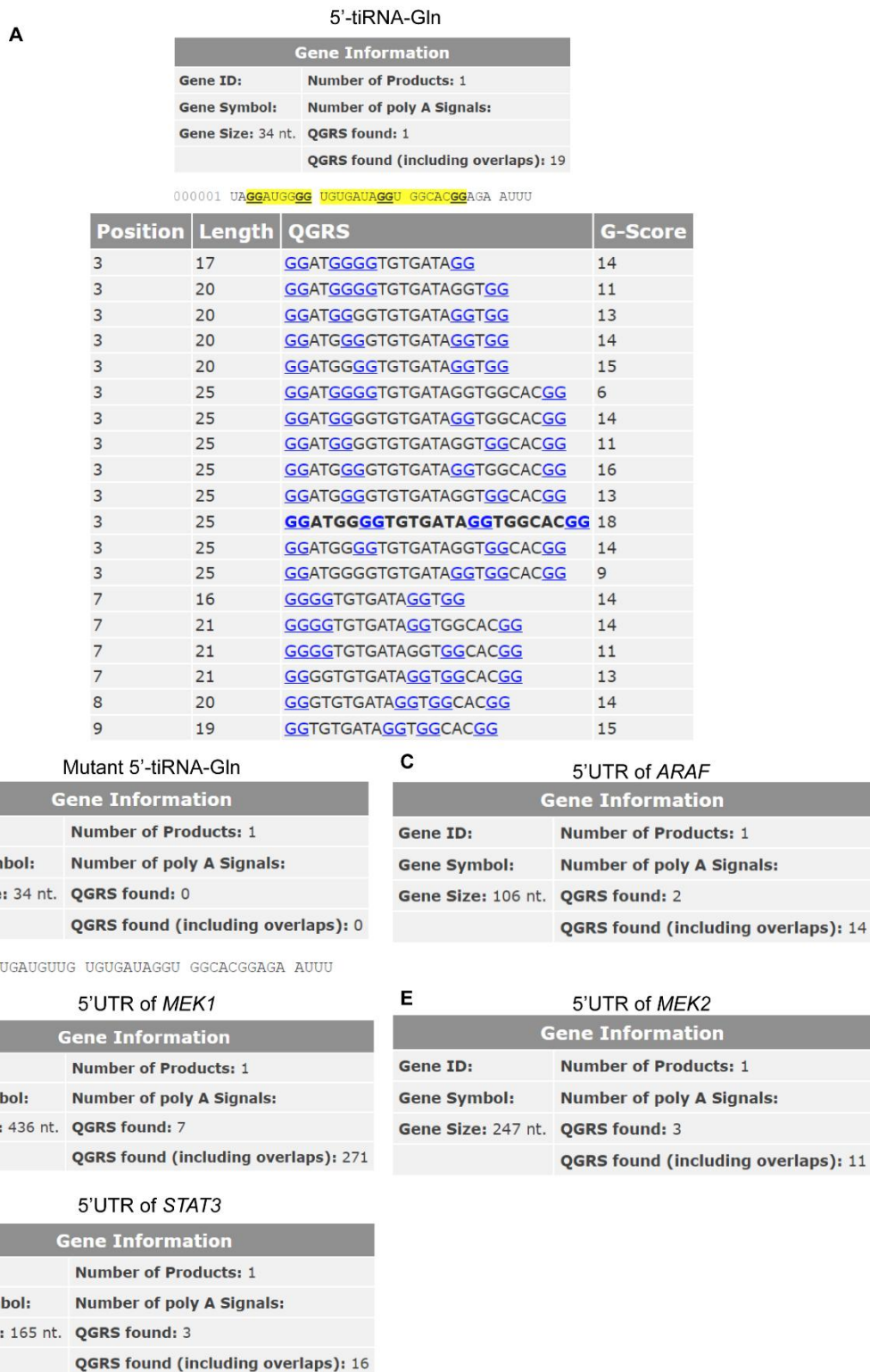


37

38

Supplementary Figure S5

39 **Supplementary Figure S5.** The downregulated proteins in HCC. **A,** The EIF4A1
40 quantity in Huh-7 cells transfected with 5'-tiRNA-Gln or control RNA. **B,** The
41 number of down- or upregulated proteins in Huh-7 cells transfected with
42 5'-tiRNA-Gln as compared to control RNA-transfected cells. **C,** Venn diagram shows
43 the intersection of the hepatitis B, hepatitis C and pathway in cancer in the KEGG
44 enrichment analysis.

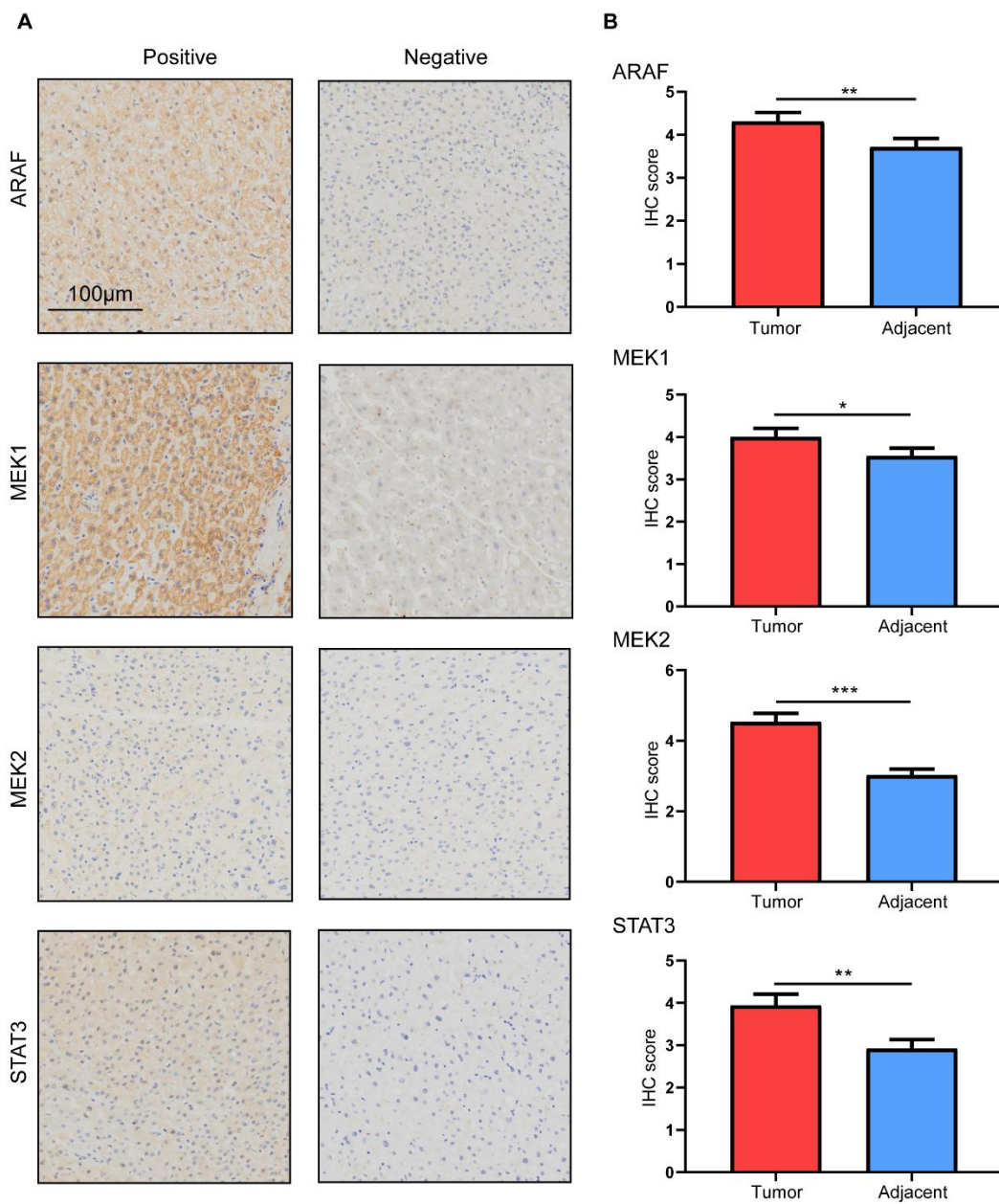


45

46

Supplementary Figure S6

47 **Supplementary Figure S6.** The G-quadruplex structure predicted by QGRS Mapper.
48 **A,** The potential G-quadruplex structure formed by 5'-tRNA-Gln (including the
49 position and sequence information of the 19 overlaps). **B,** Mutant 5'-tRNA-Gln failed
50 to form the G-quadruplex predicted by QGRS Mapper. **C, D, E, F** The number of
51 potential G-quadruplexes formed from the *ARAF* (C) *MEK1/2* (D, E) and *STAT3* (F)
52 5'-UTRs.



53

54

Supplementary Figure S7

55 **Supplementary Figure S7.** ARAF, MEK1/2 and STAT3 expression levels in the
56 adjacent nontumorous tissues. **A**, Representative IHC staining images of adjacent
57 nontumorous tissues in a microarray that included 51 paired HCC and adjacent
58 nontumorous tissue samples (scale bar: 100 μ m). **B**, Paired t-test analysis of the IHC
59 score between the paired tumor and adjacent nontumorous tissues. * $P < 0.05$, ** $P <$
60 0.01, *** $P < 0.001$.